Coating Titania Nanoparticles with Epoxy-Containing Catechol Polymers *via* Cu(0)-LRP as Intelligent Enzyme Carriers

Donghao Wang,[†,‡] Wenyi Ding,[†,‡] Kaiyue Zhou,[†,‡] Shutong Guo,[†,‡] Qiang Zhang[†,‡,] and David M. Haddleton[§]*

[†] Jiangsu Key Laboratory of Chemical Pollution Control and Resources Reuse, School of Environmental and Biological Engineering, Nanjing University of Science and Technology, Nanjing 210094, P. R. China.

[‡] Institute of Polymer Ecomaterials, School of Environmental and Biological Engineering, Nanjing University of Science and Technology, Nanjing 210094, P. R. China. Email: zhangqiang@njust.edu.cn

[§] Department of Chemistry, University of Warwick, CV4 7AL, Coventry, UK.

KEYWORDS: Intelligent nanoparticle, enzyme immobilization, bi-functional catalyst, titania, laccase, photocatalytic, enzymatic.

ABSTRACT: Immobilization of enzyme could offer the biocatalyst with increased stability and important recoverability, which plays a vital role for the enzyme's industrial applications. In this study, we present a new strategy to build an intelligent enzyme carrier by coating titania

nanoparticles with thermoresponsive epoxy-functionalized polymers. Zero-valent copper mediated living radical polymerization (Cu(0)-LRP) was utilized herein to copolymerize *N*-isopropylacrylamide (NIPAM) and glycidyl acrylate (GA), directly from an unprotected dopamine-functionalized initiator, in order to obtain an epoxy-containing polymer with terminal anchor for the "grafting to" or "one-pot" modification of titania nanoparticles. A rhodamine B-labelled laccase has been subsequently used as a model enzyme for successful immobilization to yield an intelligent titania / laccase hybrid bi-functional catalyst. The immobilized laccase has shown excellent thermal stability under ambient or even relatively high temperature above the lower critical solution temperature (LCST), at which temperature the hybrid particles could be facilely recovered for reuse. The enzyme activity could be maintained during the repeated use after recovery and enzymatic degradation of bisphenol A was proved to be efficient. The photocatalytic ability of titania was also investigated by fast degradation of rhodamine B under the excitation of simulated sunlight. Therefore, this study has provided a facile strategy for the immobilization of metal oxide catalysts with enzymes, which constructs a novel bi-functional catalyst and will be promising for the "one-pot" degradation of different organic pollutants.

Introduction

Enzymes are well known for their unique ability to catalyze ultrafast and selective reactions to produce specific materials under mild experimental conditions, which have shown extensive applications in pharmaceutical industry, biorenewables production, precision macromolecular synthesis, protein conjugation and carbon dioxide capture.[1-5] Immobilization of enzyme enhances the stability of enzyme under operational or storage conditions and facilitates efficient recycling of the biocatalyst, which is critical important for the industrial application.[6-8] Resins, biomaterials

and synthetic polymers are most frequently used supports to bind or encapsulate the enzyme in order to form an easy-handling solid phase biocatalyst for continuous production and facile separation.[9-13] Among numerous strategies to immobilize nonspecific enzymes in large scale, epoxy chemistry has drawn great attention due to the abundance of commercial epoxy supports and their ability to react with different nucleophilic groups which are abundant in the enzymes, such as amino, thiol and carboxylic groups etc.[14-19] The immobilization is believed to go through a two-step mechanism: first physical adsorption or chemical fixation of enzyme onto the support surface and followed by the intermolecular intramolecular covalent reaction of epoxy groups with the nucleophiles from the enzyme.[18, 20-22] In order to promote the adsorption of enzyme on the surface, the immobilization is often performed either under high salt concentrations or using activated epoxy-functional supports.[23, 24] The support surface could become more hydrophilic by modification of partial epoxy groups with carboxyl, boronate or copper chelate groups and this modification dramatically improved the very low reactivity of epoxy groups toward nonadsorbed enzymes.[14] Immobilization is found to be more rapid using activated epoxy-amino supports and the stability of immobilized enzyme is much higher than those using conventional epoxy supports.[15] When activated with thiol groups, the surface fixation of enzyme first takes place through effective thiol-disulfide exchange reactions followed by irreversible multipoint covalent reaction with the residual epoxy groups.[16] Recently epoxy chemistry has been applied for the immobilization of peptide/protein to microarray substrate grafted with hydrophilic epoxy-functional polymer brushes, during which the epoxy polymers showed excellent stability and high loading capacity.[25]

Intelligent enzyme carriers are stimuli-responsive materials with conformation or properties adjustable with varied pH, light, thermo, ion or magnetic parameters and have direct affection on

the properties of immobilized enzymes.[6, 7, 26-28] Such intelligent carriers have drawn much attention due to the high performance on increasing the enzyme activity, stability, loading capacity and the recoverability.[19, 21, 26-28] Novel pH-responsive polymer nanocapsules are synthesized by surface initiated reversible addition-fragmentation chain transfer (RAFT) polymerization to encapsulate enzyme myoglobin and the activity of enzyme could be controlled by adjusting the permeability of nanocapsules under different pH.[29] Hollow upconversion spheres have been constructed by DNA-mediated solvothermal strategy and coated with photosensitive compounds to realize near-infrared light controlled loading and releasing of enzymes.[30] By incorporation of thermoresponsive gels into the inner cavities of glucan microparticles, encapsulated insulin has shown much slower *in vitro* release rate and prolonged hypoglycaemic effect in both normal and diabetic rats.[31] Magnetic nanoparticles are promising enzyme supports as they can be facilely separated from the reaction mixture for reuse and great progress has been made on the preparation of magnetic polymer hybrid materials for enzyme immobilization in the last two decades.[19, 21, 32-35] Surface initiated controlled radical polymerization is very efficient on grafting high-density functional polymers from the surface for enzyme immobilization.[36-38] Surface-initiated atom transfer radical polymerization (ATRP) was utilized for the modification of nanoparticles (silica, iron oxide or polysaccharides etc.) with varied functional polymers for further loading of biomacromolecules such as peptides and DNA.[39-43] By using RAFT or Cu(0)-LRP to incorporate functional anchor groups such as phosphine or dopamine groups etc., well-defined polymers could be immobilized to the surface of iron oxide and titanium dioxide (TiO_2) nanoparticles *via* "grafting to" strategy for specific properties including glycomimetic surface, tuned LCST and antimicrobial properties.[44-47]

It is of great interest for scientists to merge the enzyme with inorganic catalysts and multi-responsive polymers to form an intelligent "multi-catalyst" system, which could be able to catalyze

different reactions in "one-pot" or treat different challenges in complex practical application.[48-52] TiO_2 is an important photocatalytic material and has been used for efficient water disinfection and degradation of certain organic pollutants.[53-55] Meanwhile, many enzymes such as laccase, horseradish peroxidase etc., can efficiently mediate the degradation of specific recalcitrant pollutants *via* precipitation or transforming process. [56-58] Laccase has been immobilized on titania nanoparticles *via* a typical cross-linking strategy and subsequently blended into the polyethersulfone membranes for water treatment applications.[59] It is the main concept of this paper to immobilize enzyme to the surface of TiO_2 nanoparticles through the attachment of thermoresponsive polymers, which forms an intelligent bi-functional catalyst for the photocatalytic and enzymatic degradation of varied pollutants in water.

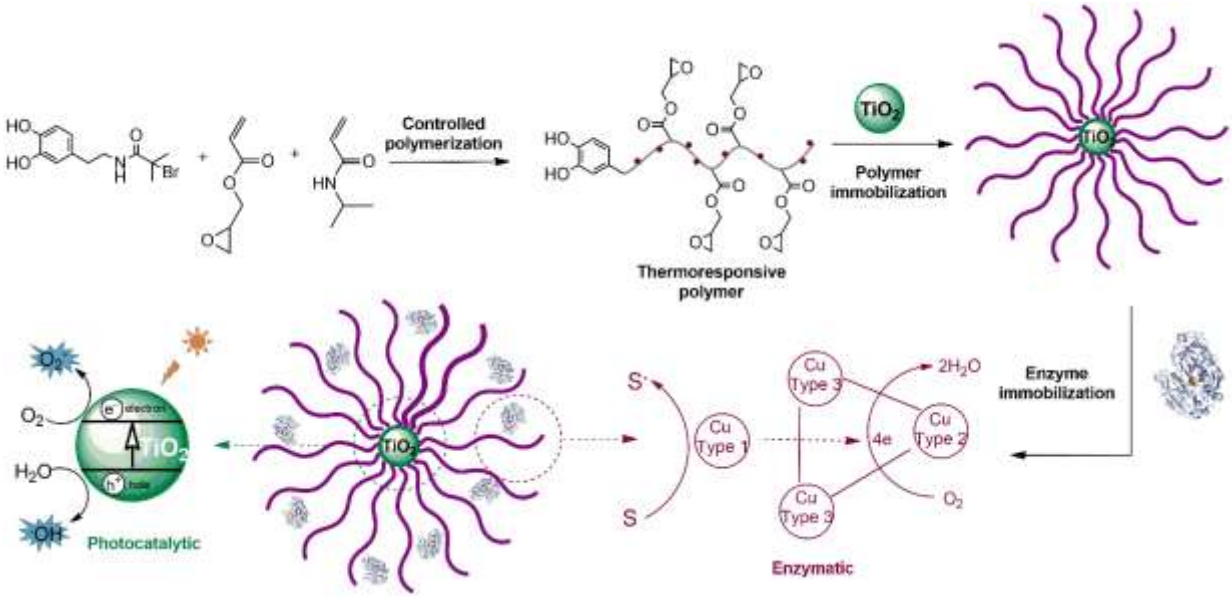

Scheme 1. Synthetic approach toward thermoresponsive TiO_2@laccase bi-functional catalyst.

As shown in Scheme 1, laccase is chosen as a model enzyme for the immobilization to the surface of TiO_2 nanoparticles *via* attachment of epoxy-functional polymers, which was hydrophilic and thermoresponsive due to the composition of typical LCST NIPAM monomer. Cu(0)-LRP is used

to synthesize the targeted polymer with terminal dopamine anchor, epoxy side group and typical LCST behaviour. The property and performance of obtained bi-functional catalyst, including the presence and catalytic performance of laccase, resistance to the environmental stressors, degradation of typical pollutants / substrates and recoverability, are systematically discussed in this research.

Experimental section

Materials

Laccase from Trametes versicolor (⩾0.5 U/mg) was supplied by Sigma-Aldrich and purified by dialysis against water for one day following lyophilization. NIPAM (97%, Aladdin) was recrystallized from hexane before use to remove the inhibitor. Glycidyl acrylate (GA), t*ris*(2-(dimethylamino)ethyl)amine (Me_6TREN), 2-bromo-N-(3,4-dihydroxyphenethy)-2-methyl propanamide (DOPA-Br) were synthesized according to literature procedure and stored in the freezer under a nitrogen atmosphere.[44, 60-62] The functional dye, rhodamine B 4-(3-(*N*-hydroxysuccinimidyloxocarbonyl)-propyl)piperazine amide (Rhod B) was synthesized according to previous procedure for the labelling of laccase directly.[63] Copper(I) bromide (CuBr, 98%, Aladdin) was washed sequentially with acetic acid and ethanol and dried under vacuum. Titanium dioxide (anatase 99.8% metals basis, average particle size: 25 nm, Aladdin) was dried in vacuum at 120 °C for 12 hours before use. 2,2'-Azobis(2-methylpropionitrile) (AIBN, 98%, Aladdin) was recrystallized from ethanol before use. Membrane dialysis (1K MWCO) was obtained from Spectrum Laboratories. All other reagents and solvents, such as 2, 2'-azinobis(3-ethylbenzothiazoline-6-sulfonic acid ammonium salt (ABTS, 98%, Aladdin) and Poly (ethylene glycol) methyl ether acrylate ($PEGA_{480}$, average M_n 480, Aladdin) etc. were obtained at the highest

purity available from Aladdin (China) and used without further purification unless otherwise stated. All polymerizations were performed under nitrogen protection using standard Schlenk technique and the stirring rate was set as 300 rpm unless otherwise stated.

Analytical techniques

SHIMADZU UV-2600 UV/Vis spectrophotometer was utilized to measure the LCST of thermoresponsive polymers at the wavelength of 500 nm and the heating rate for the thermostatically controlled cuvette was 1 °C min^{-1}. The LCST was defined as the temperature corresponding to 50% decreases of transmittance. The enzyme activity of laccase was calculated according to the degradation of ABTS in defined buffer solution and temperature using SHIMADZU UV-2600 UV/ Vis spectrophotometer to measure the absorbance at 420 nm. ^{1}H and ^{13}C NMR spectra were recorded at 25 °C with a Bruker AV 500M spectrometer using deuterated solvents obtained from Aladdin. The number-average molecular weight (M_n) and the molecular weight distribution (M_w/M_n) were determined by Waters 1515 size exclusion chromatography (SEC) in *N*, *N*- dimethylformamid (DMF) at 40 °C with a flow rate of 1.00 mL min^{-1}, which was equipped with refractive index (RI) and UV detectors, a 20 μm guard column (4.6 mm ×30 mm, 100 - 10K) followed by three Waters Styragel columns (HR1, HR3 & HR4) and autosampler. Narrow linear polystyrene standards in range of 540 to 7.4×10^5 g·mol^{-1} were used to calibrate the system. All samples were passed through 0.45 μm PTFE filter before analysis. Fourier transform infrared (FTIR) spectra were recorded on a Nicolet iS5 FTIR spectrometer using an iD7 diamond attenuated total reflectance optical base. Transition electron microscopy (TEM) images were acquired by FEI TECNAI G2 20 TEM microscope equipped with LaB6 filament. Thermal gravimetric analysis (TGA, Mettler Toledo, Switzerland) was performed at a heating rate of 10 °C min^{-1} from room temperature to 800 °C under nitrogen protection. The turbidity of the

nanoparticles were detected by WGZ-2000 turbidity meter (Beijing Warwick Industrial Science and technology, P. R. China). Fluorescence emission spectrum and life test for the solid sample was acquired from FL3-TCSPC fluorescence spectrometer (Horiba Jobin Yvon). Gas chromatography - mass spectrometry (GC-MS) was performed using a Thermo fisher spectrometer (Trace 1300-ISQ) with heating rate of GC columns increased from 50 ℃ to 200 ℃ in eight minutes. The HPLC system was an Agilent 1260 infinity series stack equipped with an Agilent 1260 binary pump, mixer and degasser. Samples were injected using an Agilent 1260 autosampler and detection was achieved using UV and fluorescence detector.

Preparation of TiO_2 / polymer hybrid nanocomposites *via* the "grafting to" strategy

The copolymerization of GA and NIPAM by Cu(0)-LRP was performed using standard Schlenk technique under nitrogen protection. The polymerization procedure is similar as previously described with addition of GA or $PEGA_{480}$ as the co-monomer.[44, 45, 64] The polymerization was monitored by ^1H NMR spectroscopy and run until a very high or even close to full conversion obtained, which cost ~ 2 h in most cases. The final polymer was purified by efficient dialysis against water for two days following lyophilization. A series of copolymers using different mole ratio of $[GA]_0$ / $[NIPAM]_0$ (defined as Rco = 0.25) or $PEGA_{480}$ monomers were synthesized in same way.

The obtained polymer (120 mg) with terminal anchor groups were then mixed with TiO_2 nanoparticles (40 mg) in deionized water (5 mL) to produce a heterogeneous suspension and stirred at 4 ℃ for two days under nitrogen protection. Final hybrid particles were isolated by centrifugation at 15 000 rpm & 4 ℃ for 15 min. After discarding the supernatant, the sediments were dispersed in cold deionized water (4 ℃) *via* sonication and were centrifuged for one more time. The above

procedure was repeated five times in order to totally remove the unreacted free polymers. Finally, the product was dried *via* lyophilization for further characterization.

Conventional radical polymerization of NIPAM and GA using AIBN as the initiator was performed in DMF under 70 ℃ for 12 h. The final random copolymer product, defined as AIBN-poly(NIPAM)-*r*-(GA) could be purified *via* dialysis against water following lyophilization. Besides, the dopamine-terminal poly(NIPAM), defined as DOPA-poly(NIPAM) was synthesized according to previous procedure.[44] As control experiments, these polymers were tried to be immobilized to the surface of TiO_2 nanoparticles using similar procedures as shown above.

"One-pot" preparation of TiO_2 / polymer hybrid nanocomposites *via* aqueous Cu (0)-LRP

The "one-pot" polymerization was performed in two vials equipped with a rubber seal and magnetic stir bar under nitrogen protection. The typical procedure is shown as below. H_2O (2 mL), Me_6TREN (26 μL, 0.1 mmol) and CuBr (14 mg, 0.1 mmol) were added into a vial for disproportionation and degassed by bubbling nitrogen into the suspension for 10 minutes. To another vial, DMF (100 μL, as internal standard to calculate the monomer conversion), H_2O (2 mL), isopropyl alcohol (i-PrOH, 2 mL), NIPAM (570 mg, 5 mmol), GA (160 mg, 1.25 mmol) and TiO_2 nanoparticles (200 mg, 2.5 mmol) were charged and degassed for 10 minutes before being transferred to the catalyst suspension *via* cannula. The polymerization was performed under ice / water cooling for one day and sample was taken at defined time during the polymerization for ^1H NMR spectroscopy in order to calculate the monomer conversion. After polymerization, the hybrid nanoparticles were separated and purified from the suspension *via* repeated centrifuge-wash cycles before lyophilization. The final product was obtained as solid powder for further characterization and test.

Fluorescent labelling of laccase by Rhod B

Laccase was labelled by Rhod B in order to prove the presence of enzyme after immobilization onto the surface of TiO_2 nanoparticles by fluorescence spectroscopy. Typically, laccase (500 mg) was dissolved in PBS buffer (pH=8, 0.1 M, 10 mL) and a solution of maleimide-functionalized Rhod B (5mg, 1.7 μmol) in DMSO (1 mL) was added dropwise. The solution was stirred for 12 hours and then stopped for dialysis against water for two days. The final Rhod B labelled laccase was recovered as pink powder *via* lyophilization.

Immobilization of laccase onto the epoxy-functionalized TiO_2 nanoparticles

TiO_2 / polymer hybrid nanoparticles (40 mg) and laccase (40mg, Rhod B labelled or not) were charged to a vial containing 5 mL phosphate buffer solution (pH=7, 0.1 M) and stirred under ambient temperature for 24 hours. The free laccase was removed *via* efficient centrifuge (15 min, 15000 rpm) and the obtained sediment particles were dispersed in deionized water and centrifuged again. The above procedure was repeated for at least 5 times. Finally, the sample is freeze-dried to yield granular products. The immobilization of laccase to the surface of TiO_2@DOPA-poly(NIPAM) was performed as control experiment in same procedure.

Activity assays of free and immobilized laccase

The enzyme activity of laccase was determined using ABTS as the substrate according to previously reported procedures by UV/Vis spectroscopy, typically measuring the absorbance at 420 nm for a defined sample after defined period and the laccase activity was deduced according to the kinetic parameters.[65] The equation used for the calculation of the activity of free laccase and immobilized laccase is shown as follow:

$$\frac{\Delta c}{\Delta t} = \frac{\Delta E / \Delta t}{36} \ [\mathbf{U\ ml^{-1}}]$$

Δc is the concentration of the sample per unit of molar concentration and $\Delta E / \Delta t$ represents the activity of absorbance change (ΔE) at a specific time interval (Δt). The extinction coefficient for the oxidation of ABTS at 420 nm is 36×10^{-3} M^{-1} cm^{-1} and the path length of the optical cell used is 1 cm. [66] 1 Unit was defined as the formation of 1 mM of product per minute.

The enzyme activity was determined under different pH (3-7), temperature (10-80 ℃) and at varied time periods (1-30 days) for both the free (60 mg/L) and immobilized (500 mg/L) laccase. To evaluate the reusability of immobilized laccase, the thermoresponsive TiO_2@laccase hybrid nanoparticles were recovered by increasing the temperature of suspension to 50 ℃, which will lead to the aggregation and precipitation of nanoparticles at the bottom of the cell. After 15 minutes, the upper-layer clear solution was removed and fresh ABTS solution was added for the next degradation cycle.

Photocatalytic and enzymatic degradation of organic pollutants in the presence of bi-functional catalyst

The degradation of Rhod B aqueous solution (20 mL, 10 mg L^{-1}, pH = 3.0) under simulated sunlight in the presence of TiO_2 nanoparticles (10 mg), laccase or hybrid bi-functional catalysts (10mg) at 50 ℃ was studied. The simulated sun light (λ = 350–780 nm) was supplied by using a 300 W xenon lamp (CEL-HXF 300, Beijing CEAULIGHT Co., Ltd, Beijing, China) equipped with a Vis-REF reflect patch. The concentration of Rhod B was measured by using UV/Vis spectrometer and all samples were filtered through a 0.45 μm PTFE filter before analysis.

The degradation of BPA aqueous solution (BPA, 20 mL, 10 mg L^{-1}, pH = 3.0) in the presence of TiO_2 nanoparticles, laccase or bi-functional catalysts were tested under both dark conditions to avoid the photocatalytic effect from TiO_2 and in the presence of simulated sunlight to verify the synergistic effect. The concentration decrease of BPA was measured by HPLC.

Results and discussion

Preparation of intelligent TiO_2@polymer hybrid nanoparticles by Cu(0)-LRP.

Herein Cu(0)-LRP was utilized for the synthesis of thermoresponsive polymer with terminal catechol anchor, which has shown well control over the molecular weight (MW) and MW distribution during the polymerization from unprotected dopamine-functionalized initiator (2-bromo-N-(3,4-dihydro-xyphenethy)-2-methylpropanamide, DOPA-Br).[44, 45] As shown in Scheme 1, GA was used as a co-monomer for the DOPA-Br-initiated copolymerization with NIPAM. However, epoxy-containing chemicals are capable of efficient ring opening reactions with varied functional groups such as thiol, amine, acid, alcohol, azide etc. and epoxy-phenol reaction is already widely used for the preparation of resins and coating materials since the early 20th century.[62, 67-71] Although the epoxide ring opening reaction could be performed with acid, thiol or amine etc. under room temperature even without the presence of catalysts, the epoxy-phenol reaction was generally performed under relatively high temperature (more than 100 ℃) or in the presence of base chemicals as the catalysts.[71-73] Before the copolymerization of GA with NIPAM, a model reaction of GA with DOPA-Br was carried out under ambient temperature to evaluate the stability of catechol groups in the presence of epoxy ring. The reaction was monitored by ^{1}H NMR and GC-MS spectroscopy.

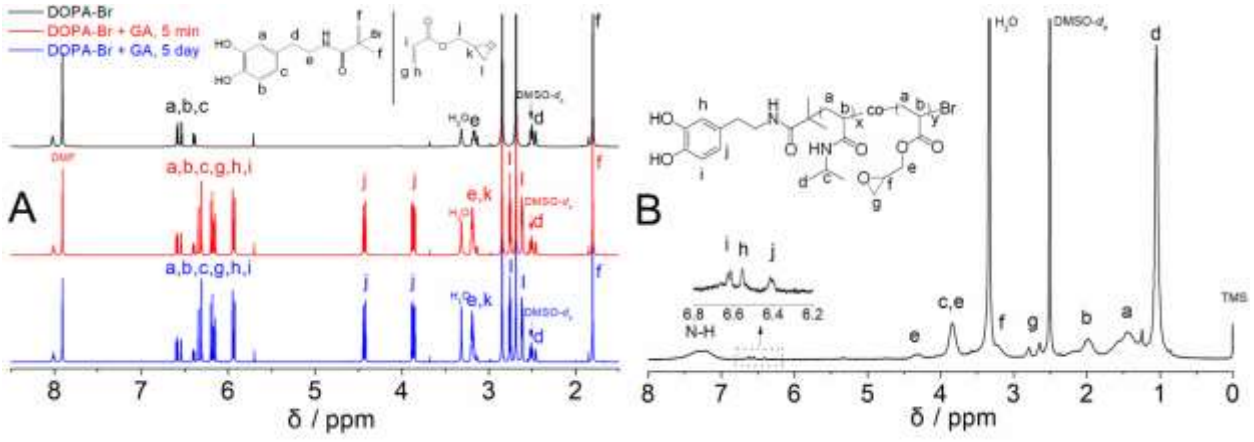

Figure 1. Evaluation of ^{1}H NMR spectra with time for the GA in the presence of DOPA-Br in DMSO-d_6 at 25 ℃ (**A**, DMF as internal standard) and the ^{1}H NMR spectrum of poly(NIPAM)-*r*-(GA) (R_{co}=0.1) in DMSO-d_6 (**B**).

As shown in Figure 1, the signals at 6.6-6.8 ppm (the three protons from benzene ring of the DOPA-Br), 5.8-6.2 ppm (vinyl groups from GA) and 2.6-3.2 ppm (three protons from the epoxy ring of GA) still existed even after addition of GA for 120 hours. No significant new peaks could be detected, which indicated that the epoxy ring opening reaction with catechol group did not happen under previous reaction conditions or could not be detected by NMR spectroscopy, either due to the low reaction conversion or overlap of similar resonance between the reactants and products. This result is in accordance with previous reports on the epoxy-phenol reaction conditions.[71, 73] Subsequently we used GC-MS (Figure S 1) to analyse the composition of GA and DOPA-Br mixture after reaction for 120 hours under ambient temperature. As shown in Figure S 1, GC revealed the presence of original GA and DOPA-Br at 8.5 min and 13.8 min separately as well as the appearance of new small peaks at 10.3 min, which was ascribed to ring-opening products of GA with activated hydrogen according to MS calculation. However, it is worth noting that the GC-MS test was performed under relatively high temperature (up to 200 ℃), which may

accelerate the epoxide ring opening reaction with phenols. Nevertheless, these results prove that catechol groups are stable in the presence of epoxy-functional monomers under ambient temperature, which is close to the polymerization conditions of Cu(0)-LRP.

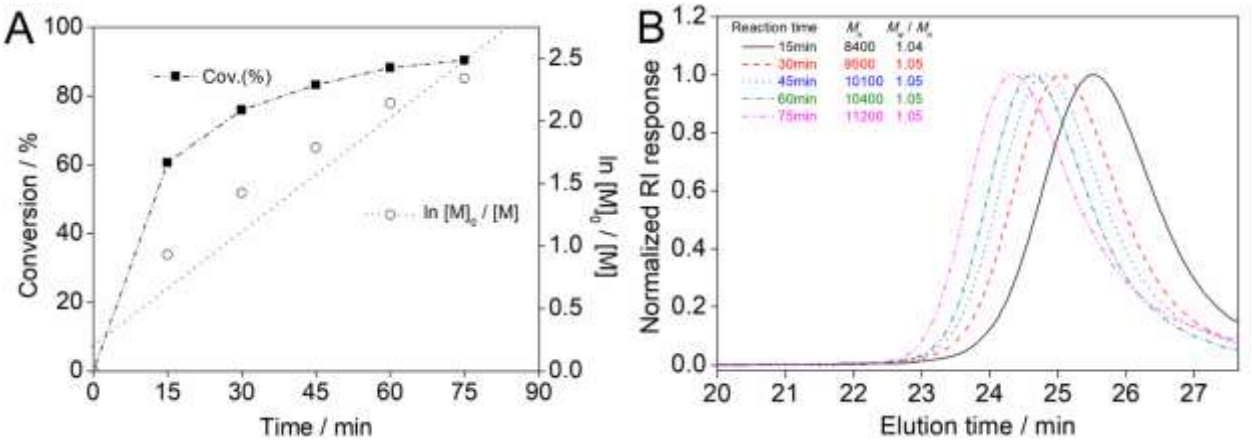

Figure 2. Conversion and ln([M]$_0$/[M]) *vs* time plots (**A**) and SEC elution traces (**B**) for the Cu(0)-LRP random copolymerization of NIAPM and GA in i-PrOH/H_2O (R_{co}=0.1).

The copolymerization of GA and NIPAM by Cu (0)-LRP was first performed in water / i-PrOH solution using CuBr / Me_6TREN as the pre-catalyst in the following conditions: [DOPA-Br]: [NIPAM]: [GA]: [CuBr]: [Me_6TREN] = 1: 20: 2: 0.4: 0.4. The polymerization went fast with a conversion of 90% for NIPAM and a conversion of 93 % for GA obtained in 75 minutes. SEC revealed a gradual increase of MW from 8400 Da to 11200 Da and the dispersity value remained relatively narrow (M_w/M_n = ~ 1.05) until conversion reached more than 90% as shown in Figure 2. However, several shoulder peaks appeared when the polymerization was left for 19 hours after high conversion was obtained (Figure S 2). Although radical-radical coupling termination reactions are very common in controlled radical polymerizations, it is hypothesized that these shoulder peaks are possibly caused by the side reactions of epoxy and catechol groups. Thus the polymerizations by Cu (0)-LRP were often terminated after 2 h in order to avoid the side reactions

while attaining very high conversions. ^{1}H NMR spectrum (Figure 1 B) of the final product (terminated after polymerization for 2 h) revealed typical resonances of poly(NIPAM) at 1.2 ppm (for protons from the methyl groups) and 4.1 ppm (for protons from the methine groups). The presence of epoxy-functional polymers was proved by the resonance at 4.4 ppm (for protons from the methylene groups close to the ester bond) and 2.7 & 2.8 ppm (for protons from the methylene groups of epoxy ring). The resonance at 6.4-6.7 ppm were from the three protons of terminal catechol groups and the average MW (4106 Da) of final polymer was calculated as by comparing the integral of catechol residues with typical peaks of NIPAM and GA, which is ~ 46 % higher than the theoretical MW (2818 Da). This deviation was due to the relatively low initiator efficiency of DOPA-Br with amide bond, which may cause certain radical termination at the early period of polymerization.[44, 74] The presence of epoxy polymer was also proved by the peak at 1750 & 906 cm^{-1} in the FTIR spectra (Figure 3 D) of the final polymer, which was attributed to the ester bond and epoxide ring. Besides, SEC system using DMF as the eluent and narrow distributed polystyrene as the standard polymer also revealed much higher MW than the theoretical value, possibly due to the different hydrodynamic volume of obtained polymers, which has also been observed in the previous reports. [44, 64]

It is worth noting that the epoxy groups are able to react with nucleophilic groups (e.g., thiol, amine), however, the epoxy groups are hardly reactive under mild reaction conditions as previously reported.[15] Although the epoxy polymers were often exposed to aqueous condition for days during the post-polymerization treatment, clear presence of epoxy groups could be found as shown in the ^{1}H NMR spectra (Figure 1 B) of the final product. To further check the hydrolysis rate of glycidyl groups during the synthesis and purification of functional polymers, homopolymer poly(GA) synthesized by Cu(0)-LRP was immersed in water or even slightly alkaline solution

(PBS buffer, pH=8.0, 0.1 M) for up to a week.[62] As shown in the ^{1}H NMR spectra (Figure S 3), no epoxide ring opening reaction was found as the resonances of typical groups from the polymer before and after the treatment were the same, which demonstrates that the epoxide groups are stable under aqueous conditions and its hydrolysis was not significant.

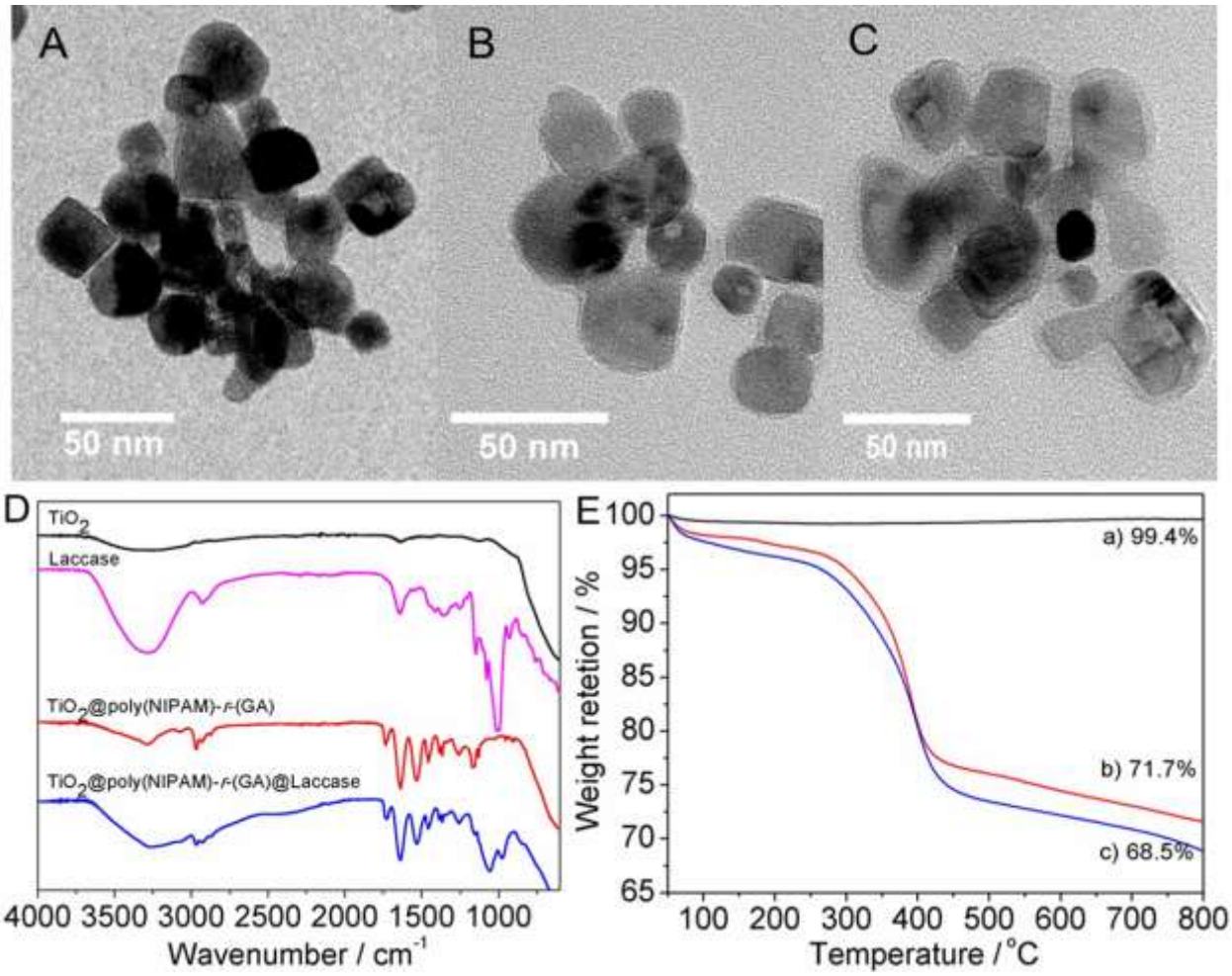

Figure 3. TEM images (**A**, **B**, **C**), FTIR spectra (**D**) and TGA (**E**, R_{co}=0.25) of TiO_2 (A & a), TiO_2@poly(NIPAM)-*r*-(GA) (B & b, R_{co} = 0.25) and TiO_2@poly(NIPAM)-*r*-(GA)@Laccase (C & c, R_{co} = 0.25) nanoparticles.

Subsequently the catechol-terminal epoxy polymer (poly(NIPAM)-r-(GA), R_{co} = 0.25) was used for the surface functionalization of TiO_2 nanoparticles. TEM images (Figure 3 A & B) demonstrate the presence of a thin polymer layer on the particle surface. The FTIR spectrum (Figure 3 D) of

TiO_2 @poly(NIPAM)-*r*-(GA) showed clear peaks of NIPAM at 1640.6 cm^{-1} (C=O stretching) and 1538.9 cm^{-1} (N–H in-plane bending vibration) as well as the absorbance from GA at 1739.5 cm^{-1} (C=O stretching) and 1165.8 cm^{-1} (C-O-C stretching). TGA analysis (Figure 3 E) revealed a weight loss of only 0.6% for the raw TiO_2 nanoparticles yet up to 28.3% after immobilization of epoxy polymers. All these results proved the successful preparation of TiO_2@ poly(NIPAM)-*r*-(GA) *via* "grafting to" strategy.

To prove the attachment of polymer to the surface of TiO_2 nanoparticles through terminal dopamine group, a control experiment was performed using a random copolymer poly(NIPAM)-*r*-(GA) synthesized by conventional radical polymerization. The AIBN initiated polymerization induced to AIBN-poly(NIPAM)-*r*-(GA) without terminal catechol group and broad MW distribution (Figure S 4), which was subsequently used for surface functionalization of TiO_2 nanoparticles. As shown in Figure S 5, the FTIR spectra of TiO_2@ AIBN-poly(NIPAM)-*r*-(GA) revealed almost the same absorbance as that of the pristine TiO_2. Very weak absorption band from the copolymer could be observed, indicating the presence of certain copolymer on the surface of nanoparticles. However, the intensity of absorption band is very weak compared with that from the TiO_2@DOPA-poly(NIPAM)-*r*-(GA), as shown in Figure S 5. TGA analysis showed similar thermogravimetric degradation for the TiO_2 and TiO_2@ AIBN-poly(NIPAM)-*r*-(GA) and loss of weight is only 0.6% and 4.1% separately, which is much lower than that of TiO_2@DOPA-poly(NIPAM)-*r*-(GA) (up to 28.3%). All these results strongly prove that the attachment of copolymer is mainly through the strong interaction between TiO_2 and catechol groups. The physical adhesion or intermolecular interactions between TiO_2 and copolymers tend to be weak and almost could be overlooked compared with the strong catechol-TiO_2 interaction.

In the previous report, a "one-pot" strategy has been used for simultaneous polymerization and post modification in order to avoid the multi-step purification procedures.[45] It is hypothesized that this strategy may help to reduce the side reactions between the epoxy ring and catechol groups, mostly due to the high reactivity of catechol groups toward TiO_2. Thus TiO_2 nanoparticles were directly added into the system at the beginning of the reaction for one polymerization conducted under the following reaction conditions: [DOPA-Br]: [NIPAM]: [GA]: [CuBr]: [Me_6TREN] =1: 20: 2: 0.4: 0.4. ^{1}H NMR spectroscopy (Figure S 7) was used to monitor the polymerization and it showed that a conversion of 93% could be obtained after two hours. Several polymerizations using varied monomer compositions were performed with all high conversion (even close to full conversion) and well-controlled MW and MW distributions obtained in short reaction time. The free linear polymers were isolated from the titania nanoparticles *via* centrifuge for further characterization. SEC (Figure S 8) revealed the presence of well-defined polymer with relatively low MW and narrow distribution in the solution and a relatively high MW peak was also observed, which was similar as previous report and was attributed to the fast polymerization initiated by possible excess catalysts.[45] It has been observed that "grafting to" strategy often leads to lower grafting density due to the steric effect compared with the "grafting from" strategy. The "one-pot" strategy utilized here is in actual fact a combination of "grafting to" and "grafting from" strategy. Thus the hybrid nanoparticles prepared by "one-pot" strategy could theoretically load more polymers on the surface. As shown in the TGA analysis (Figure S 9), it showed a weight loss up to 33.7%, which is indeed higher than that obtained from the "grafting to" strategy. Based on the size (~ 25 nm), density of TiO_2 nanoparticles and the TGA results as well as the MW of immobilized polymers, we can calculate the grafting density is ~ 0.26 and 0.33 chains nm^{-2} separately for the nanoparticles obtained by "grafting to" and "one-pot" strategies.

The final TiO_2@poly(NIPAM)-*r*-(GA) nanoparticles showed different thermo phase transition behaviours and the LCST also changed significantly with the increase of R_{co}. As shown in Figure 4 A, the absorbance of the suspension (TiO_2@poly(NIPAM)-*r*-(GA) nanoparticles in water, 1 mg/mL) sharply increased when the temperature was above the LCST of the polymer. This indicates that above the LCST the polymer becomes insoluble in water and interchain aggregation happens, further leading to the aggregation of nanoparticles, which will scatter the incident light and decrease the optical transmittance. One interesting phenomenon was also observed that with the increase of R_{co} from 0.125 to 0.5 the aggregation temperature (defined as the temperatures corresponding to 50% decreases of transmittance) of TiO_2@polymer nanoparticles starts to decrease from 38 ℃ to 25 ℃, which is mostly due to the increase of hydrophobic GA composition. To extend the temperature responsive zone of the TiO_2@polymer nanoparticles, more hydrophilic monomer such as poly(ethylene) glycol methyl ether acrylate, was used as the co-monomer for polymerization (SEC & ^{1}H NMR spectrum, Figure S 8 & 10) and the thermo-induced aggregation temperature of obtained hybrid nanoparticles increased to ~ 50 ℃ (Figure 4 A). This indicates that the aggregation temperature of final nanoparticles could be well-tuned by changing the monomer composition of epoxy-functional polymers. The difference in the initial absorbance of varied nanoparticles (10 ℃, Figure 4 A) may be due to the different grafting density and solubility of grafted polymers, which will lead to the presence of different amounts of hybrid nanoparticles even under same concentration as well as different setting velocity. In summary, TiO_2 nanoparticles have been successfully coated with thermoresponsive epoxy-functional polymers *via* "grafting to" or "one-pot" strategy using Cu(0)-LRP.

Immobilization of laccase onto the epoxy-polymer-functionalized TiO_2 nanoparticles

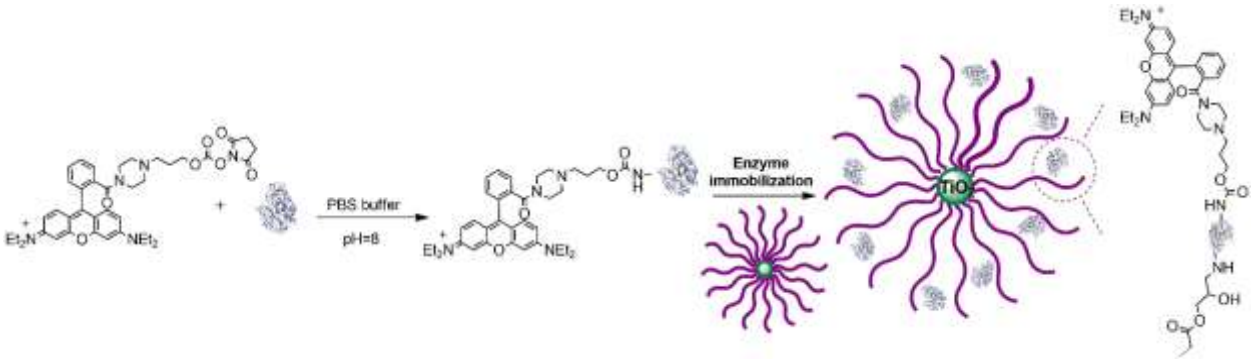

Scheme 2. Fluorescent labelling of laccase by Rhod B for the immobilization to epoxy-functionalized TiO_2 nanoparticles.

Laccase was then immobilized to the surface of TiO_2@polymer hybrid nanoparticles *via* the reaction of epoxy groups with the nucleophiles exposed on the enzyme surface. In order to prove the successful immobilization, laccase was first labelled by a maleimide-functionalized rhodamine dye (Scheme 2) so that the modification could be characterized *via* fluorescence spectroscopy or even visually. The enzyme activity (Figure S 11) only slightly decreased from 0.51 U mg^{-1} to 0.49 U mg^{-1} after the fluorescent labelling, mainly due to the low content of induced dye. The immobilization of enzyme was performed in PBS buffer (pH=7, 0.1 mmol/L) at ambient temperature.

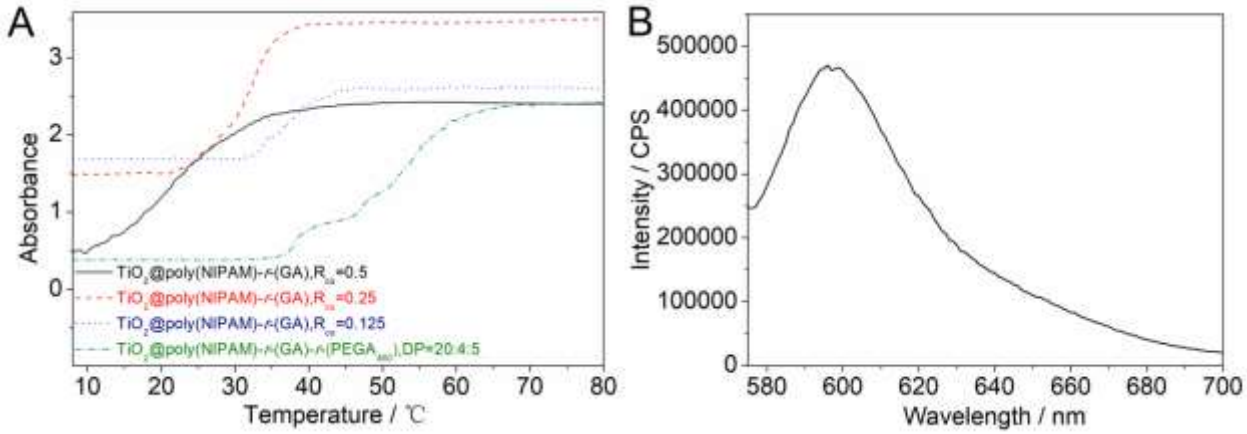

Figure 4. Temperature dependence of absorbance at 500 nm obtained for the aqueous suspensions of TiO_2 / polymer hybrid nanoparticles (**A**, 1 mg/mL, all by "grafting to" strategies) and fluorescence spectroscopy (**B**) of TiO_2@poly(NIPAM)-*r*-(GA)@Rhod-laccase (R_{co}=0.25).

As shown in the TEM images (Figure 3 C), the layer of soft matter on the particle's surface tends to become thicker and much clearer after immobilization of enzyme, indicating the success of subsequent modification. The FTIR spectra demonstrate typical peaks from laccase at ~ 3300 & 1100 cm^{-1} as well as peaks related to the polymer from 1200-1800 cm^{-1} (Figure 3D). TGA analysis (Figure 3 E) reveals an increase of weight loss from 28.3% to 31.5% after enzyme immobilization, which is caused by the addition reaction of laccase and demonstrates that the laccase loading is 3.2 wt% thus the enzyme loading amount is ~ 32 μg/mg support, which is much higher than that (8.6±1.0 μg/mg) in previous report using small molecular cross-linkers for immobilization.[59] After reaction the products were obtained as pink powders, although the composition of rhodamine B in the enzyme was low, the hybrid biocatalyst exhibited high fluorescence intensity at ~ 595 nm upon irradiation (λ_{ex} = 565 nm, Figure 4 B). These results proved the successful immobilization of enzyme to the surface of TiO_2 nanoparticles and the loading yield is similar as previous reports using commercial resin beads.[16]

To further prove the covalent attachment of enzyme on the polymeric surface rather than the physical adsorption, a control experiment using epoxy-free TiO_2 / DOPA-poly(NIPAM) hybrid nanoparticles was performed for the immobilization of enzyme. DOPA-poly(NIPAM) was synthesized by homo-polymerization of NIPAM using dopamine-functionalized initiator.[44] FTIR and TGA were used for the characterization of final products. As shown in Figure S 12, the FTIR spectra did not reveal significant changes after enzyme immobilization. The TGA curves (Figure S 13) for the TiO_2@DOPA-poly(NIPAM) nanoparticle before and after enzyme immobilization

were almost overlapped and the weight loss (9.8%) was very close to that (9.5%) from the unmodified TiO_2@DOPA-poly(NIPAM). Such small differences could be from the errors during the measurement or caused by the presence of tiny physically absorbed enzyme, which indicated no significant occurrence of conjugation. All these results prove that the enzymes are covalently attached to the hybrid nanoparticles *via* epoxy chemistry rather than physical adsorption.

Stability, reusability and catalytic performance of bi-functional catalyst

Epoxy-functionalised copolymer has shown different water solubility and LCST in water, which mainly depends on the composition ratio of hydrophilic monomers (NIPAM, $PEGA_{480}$) to hydrophobic monomer (GA). The sedimentation of unmodified TiO_2 nanoparticles in water goes fast and most of the particles could precipitate at the bottom under ambient temperature in 30 minutes (Figure 5 A). After coating with functional copolymers, the hybrid TiO_2 nanoparticles have shown better dispersion stability in water and the sedimentation rate is much slower as visually observed (Figure 5 A) or by turbidity characterization (Figure S 14). When the temperature is above the LCST, significant aggregation between the hybrid particles could be observed and most of the particles already precipitate in 10 minutes (Figure 5 B).

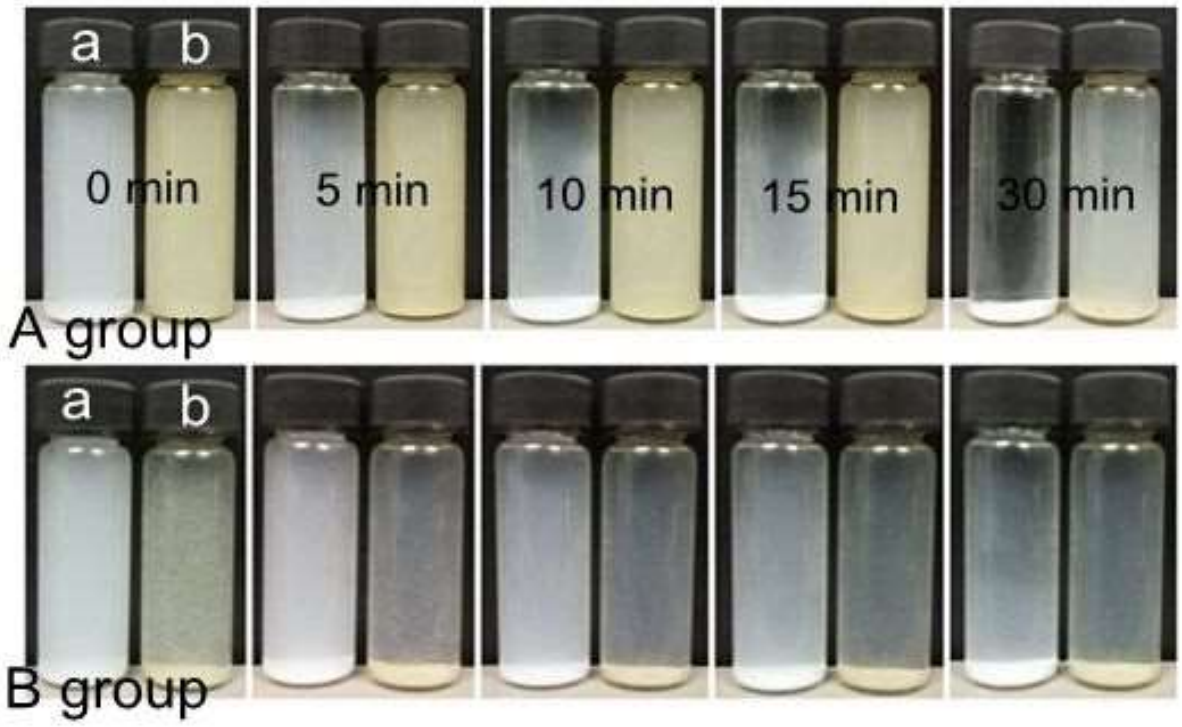

Figure 5. Optical photographs of TiO_2 (a) and TiO_2@poly(NIPAM)-*r*-(GA) (b, R_{co}=0.25, obtained by "grafting to" strategy) hybrid nanoparticles in aqueous solution at 25 ℃ (**A** group) or at 50 ℃ (**B** group). Photographs were taken at 0, 5, 10, 15 and 30 minutes respectively (from left to right).

Due to the presence of LCST polymer, which will cause aggregation under stimuli of high temperature to encapsulate the enzyme with a "polymer coat", it is hypothesized that the enzyme stability will be increased after immobilization especially under relatively high temperature. The enzyme activity is calculated by measuring the degradation of ABTS in the PBS buffer solution (0.2 M) by UV/Vis spectroscopy under different pH (ranging from 2 to 7) and temperature (ranging from 10 to 80 ℃). The optimum pH and temperature for the free laccase was determined as pH =3.0 and 50 ℃. After being attached to the TiO_2 nanoparticles, the immobilized laccase also shows the highest activity at pH=3.0 and 50 ℃ (Figure 6). However, the enzyme activity of immobilized laccase decreased to ~ 60% of that from the free laccase, indicating the effect of conjugation on

the activity of enzyme. It is hypothesized that the chemical modification and steric effect due to the presence of polymer may change the spatial conformation of enzyme and affect the binding of enzyme with substrates. It is worth noting that the enzyme activity recovery (~ 60%) for the immobilized laccase under a much higher enzyme loading amount in this research is higher than that in previous report using glutaraldehyde as cross-linkers.[59] It also needs to be emphasized that the activity of laccase significantly decreased when the temperature was increased to 60 ℃ or higher, however, the free laccase decreased much faster than the immobilized laccase as shown in Figure 6. This further demonstrates the importance of thermoresponsive polymers on the maintaining of enzyme activity. We believe that the polymer coat will embrace the enzyme inside and prevent the enzyme from subunit dissociation or denaturation during heating.

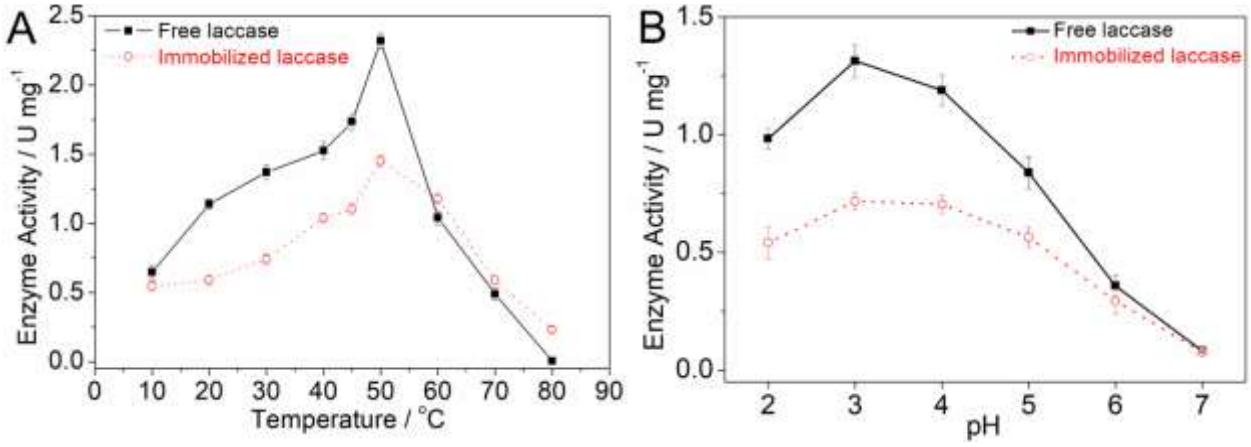

Figure 6. Enzyme activity of free and immobilized laccase (TiO_2@poly(NIPAM)-*r*-(GA))@Laccase, R_{co}=0.25) under different temperature (**A**, the pH was set as 3.0) and pH (**B**, the temperature was set as 25 ℃).

The stability of enzyme has always been a key concern during enzyme's industrial application. Figure 7 shows the relative activity of the free and immobilized laccase in PBS buffer (pH=3, 0.2 M) under 25 ℃ after different periods. Both samples show a decrease of relative activity with the

increase of time and it is worth noting that the relative activity of free laccase decreased fast to ~60% after one day, only 10% left after 5 days and 0% after 15 days, indicating a fast loss of activity. However, the immobilized laccase keeps 96% of activity after one day, ~ 50% after 5 days and even ~ 10% left after four weeks, which demonstrates much better stability through storage after immobilization.

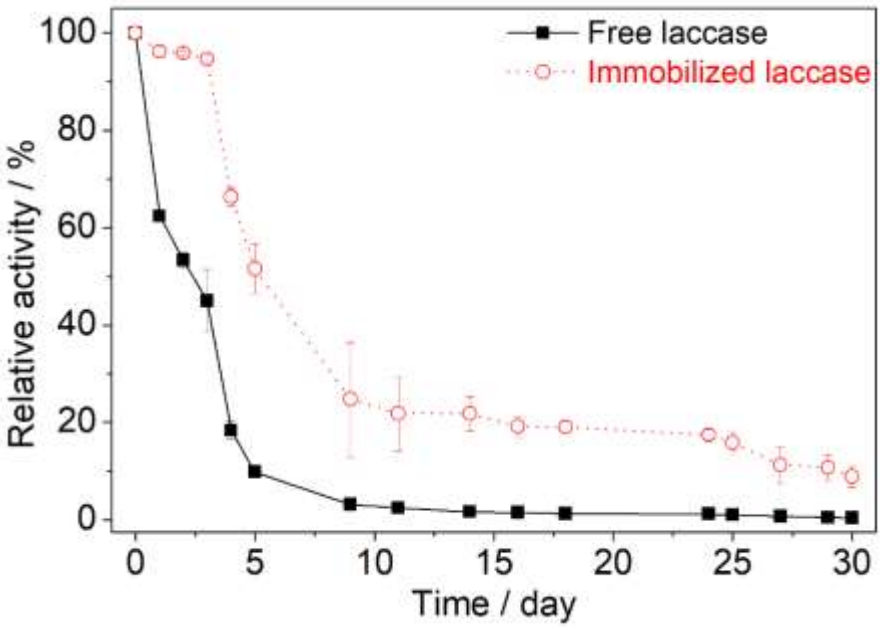

Figure 7. Relative activity of the free and immobilized laccase (TiO_2@poly(NIPAM)-*r*-(GA))@Laccase, R_{co}=0.25) incubated in PBS buffer (pH=3, 0.2 M) under 25 ℃ at different time.

The increase of temperature can disrupt the hydrogen bonds in the protein and change the advanced structures (secondary, tertiary and quaternary structure), which leads to the denaturation of protein and loss of activity or function. A significant decrease of activity is observed when the temperature is increased to higher than 60 ℃ (Figure 6). When laccase was heated to 80 ℃, fast loss of activity was found and less than 10% of activity could be maintained after 2 hours, only ~ 2% left after 4 hours (Figure 8) and total loss of activity after 24 hours. Decrease of activity under high

temperature is also observed for the immobilized laccase; however, the declining rate is much slower compared with pristine laccase and ~ 30% of activity is maintained after 2 hours, ~ 20% left after 4 hours and even ~ 4% of activity left after 24 hours. These results further prove the increased stability for the immobilized laccase even under relatively high temperature.

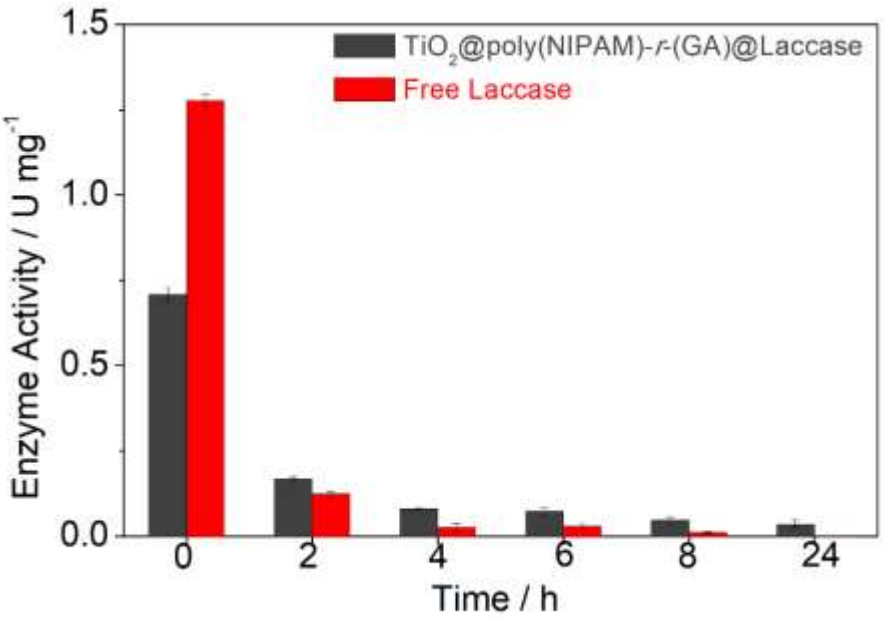

Figure 8. The effect of temperature on the free and immobilized laccase (TiO_2@poly(NIPAM)-*r*-(GA))@Laccase, R_{co}=0.25).

The reusability of immobilized laccase was calculated by measuring the enzyme activity through the degradation of ABTS, during which the TiO_2@polymer@laccase catalyst was separated from the system before next cycle *via* increasing the temperature to the one above the LCST for efficient flocculation. As shown in Figure 9, the enzyme activity dropped ~ 20% through the first three cycles. It is hypothesized that a part of the hybrid nanoparticles, especially the one with relatively smaller size, may cannot be efficiently recovered during the temperature-induced flocculation. It is also possible that the enzyme was gradually destroyed in use thus the activity dropped.

However, the rest catalysts maintained relatively stable activity during the subsequent 4 recycles, which exhibited good reusability and retained ~ 60% residual activity after 8 total cycles. In summary, the immobilized laccase could be efficiently recovered *via* thermo-control and reused with high activity maintained.

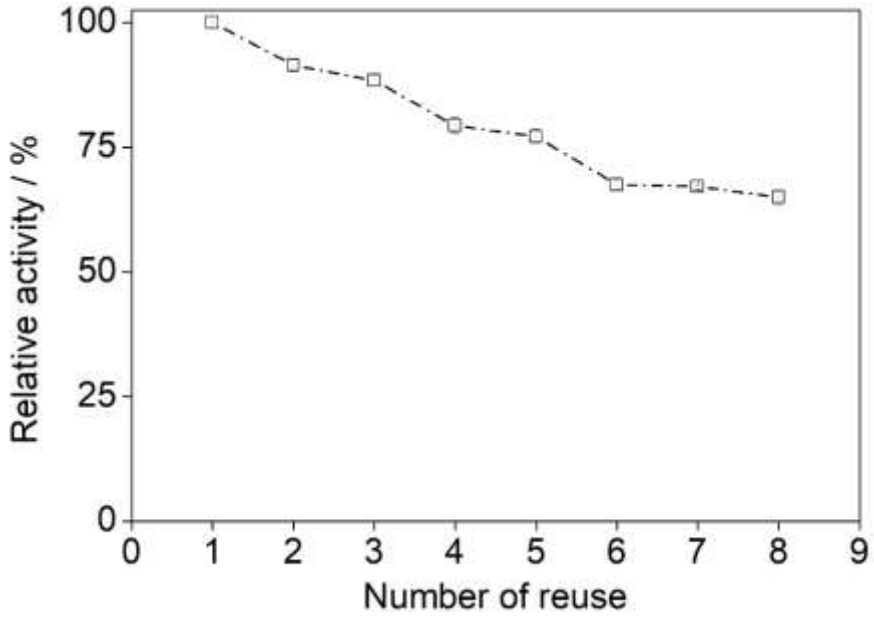

Figure 9. The operation stability of immobilized laccase (TiO_2@poly(NIPAM)-*r*-(GA))@Laccase, R_{co}=0.25).

The bi-functional catalysts are composed by photocatalytic TiO_2 nanoparticles and enzymatic laccase, which have shown wide applications in the degradation of organic pollutants such as formaldehyde, dye and phenolic chemicals etc.[75-78] The catalytic performances of the bi-functional catalyst are briefly evaluated in this paper by degradation of rhodamine B (Rhod B) and bisphenol A (BPA). As shown in Figure 10A, the degradation of Rhod B was performed under simulated sunlight with control experiments to verify the role of TiO_2 and laccase. It showed that the photodegradation of Rhod B could happen even in the absence of catalysts and a degradation ratio

of ~ 40% could be obtained in 150 minutes. Interestingly, the addition of laccase could adversely affect the degradation of Rhod B as only ~ 10% of degradation could be obtained in 150 minutes. Nevertheless, the degradation went much faster with the addition of TiO_2 nanoparticles or the TiO_2@poly(NIPAM)-*r*-(GA)-*r*-($PEGA_{480}$) hybrid nanoparticles, for which the degradation ratio could go to up to 95% and 75% separately in 30 minutes and both close to 100% in 90 minutes. Interestingly, the degradation of Rhod B in the presence of TiO_2@poly(NIPAM)-*r*-(GA)-*r*-($PEGA_{480}$)@Laccase went much faster than that in the presence of TiO_2@poly(NIPAM)-*r*-(GA)@Laccase. It is hypothesized that the utilized temperature (50 ℃) is higher than the LCST of poly(NIPAM)-*r*-(GA) and leads to the aggregation of nanoparticles, which may cover the active sites of TiO_2 thus decrease the enzyme activity. While the aggregation of TiO_2@poly(NIPAM)-*r*-(GA)-*r*-($PEGA_{480}$)@Laccase nanoparticles only occurred partially under 50 ℃ thus the degradation of Rhod B went much faster. When the degradation was performed under decreased temperature at 25 ℃, the degradation of Rhod B in the presence of TiO_2@poly(NIPAM)-*r*-(GA)@Laccase became faster than that under 50 ℃ (Figure 10 A). This further revealed that the thermoresponsive polymers under LCST will not cover the active sites of TiO_2 thus favoured the photodegradation of Rhod B. For the degradation in the presence TiO_2@poly(NIPAM)-*r*-(GA)-*r*-($PEGA_{480}$)@Laccase, the degradation rate became a bit slower when the temperature was decreased from 50 ℃ to 25 ℃. This is in agreement with our previous finding that the degradation of Rhod B is temperature-relevant and higher temperature will accelerate the degradation.[45] All these results suggest that the photocatalytic ability of TiO_2 has been maintained even after being coated with a dense polymer and laccase layer.

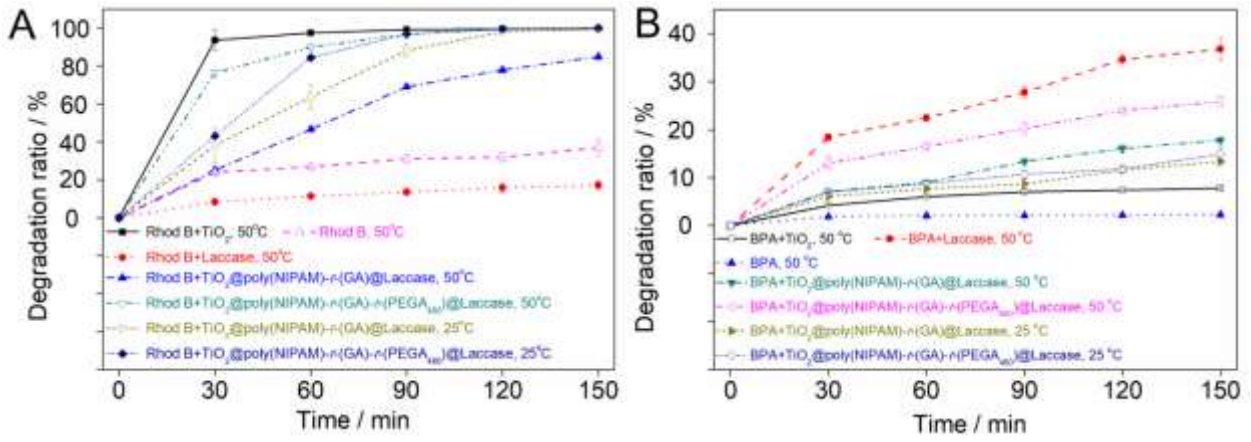

Figure 10. Degradation of Rhod B (10 mg/L, under the irradiation of simulated sunlight, **A**) and BPA (10 mg/L, under dark condition, **B**) in the presence of TiO_2, TiO_2@poly(NIPAM)-*r*-(GA)@Laccase (R_{co}= 0.25) and TiO_2@poly(NIPAM)-*r*-(GA)-*r*-($PEGA_{480}$)@Laccase nanocomposites (DP = 20:5:4) at 50 ℃ in PBS buffer (pH=3, 0.2 M). The concentration of all the particles in the suspension is 0.5 mg / mL.

After that, the activity of immobilized laccase was measured by catalysing the degradation of BPA. The experiments were performed under dark conditions as the photocatalytic degradation of BPA has been reported to occur under the presence of TiO_2 catalyst.[76] The degradation of BPA in the absence of catalyst is very slow; however, after addition of pristine TiO_2 nanoparticles for 150 minutes the concentration of BPA decreased by ~ 5% (Figure 10 B). It is worth noting that the phenol groups have strong interactions with TiO_2 and may increase the agglomeration and zeta potential of nanoparticles.[79] The adsorption capacity of BPA by TiO_2 nanoparticles could be up to 0.2 mmol/g and should not be ignored in this research as it significantly contributes to the concentration decrease of BPA. Nevertheless, the degradation of BPA catalysed by laccase has shown the fastest rate and ~ 40% of BPA has been degraded in 150 minutes. The degradation of BPA in the presence of TiO_2@poly(NIPAM)-*r*-(GA)-*r*-($PEGA_{480}$)@laccase is much faster than

that in the presence of pristine TiO_2 or blank control experiment and only slightly slower than that in the presence of free laccase, which demonstrates that the immobilized laccase could efficiently catalyze the degradation of BPA. It is also worth noting that the enzymatic degradation of BPA in the presence of TiO_2@poly(NIPAM)-*r*-(GA)@Laccase under 50 ℃ is also slower than that in the presence of TiO_2@poly(NIPAM)-*r*-(GA)-*r*-($PEGA_{480}$)@laccase, probably also due to the thermo-induced aggregation between the nanoparticles, which will unavoidably cover some active sites of laccase. Nevertheless, this temperature-responsive behaviour suggests that the catalyst could be recovered and the catalytic activity could also be tuned with change of temperature. Moreover, the degradation of BPA became much slower when the temperature was decreased from 50 ℃ to 25 ℃, which indicates that the enzymatic activity could be seriously affected by temperature.

For the degradation of BPA in the presence of bi-functional catalyst under simulated sunlight, the degradation rate tends to be even faster than that in the presence of only TiO_2 or laccase, which revealed a synergistic effect for the simultaneous photocatalytic and enzymatic degradation of BPA (S Figure 8). All these results prove the efficiency of bi-functional catalysts and show advantages on enzyme storage, stability, reusability and synergistic degradation of typical organic pollutants, which will be promising for the applications in the environmental science and biomaterials area.

Conclusions

In conclusion, we have successfully immobilized laccase onto the surface of TiO_2 nanoparticles through the linkage of thermoresponsive epoxy-functional polymers. Cu(0)-LRP of GA and NIPAM has shown typical characteristics of living radical polymerization even in the presence of catechol-functionalized initiator, yielding epoxy-containing polymers with terminal anchor for the

surface modification of TiO_2 nanoparticles *via* "grafting to" or "one-pot" strategies. The successful immobilization of enzyme has been proved by the presence of fluorescent laccase after the epoxide ring-opening reaction with nucleophiles from the laccase, using different characterization tools such as FTIR, TGA, TEM and fluorescence spectroscopy. The synthesized bi-functional catalyst has shown different disperse behaviour in aqueous solution depending on the composition of copolymers and could be facilely recovered for reuse when the temperature is higher than the corresponding LCST. The immobilized laccase has shown excellent thermal stability under ambient or even relatively high temperature compared with the free laccase. The enzyme activity could be maintained during the repeated use after recovery and enzymatic degradation of BPA was proved to be efficient. The photocatalytic ability of TiO_2 was also investigated by fast degradation of rhodamine B under the excitation of simulated sunlight. Moreover, the strategy developed herein could be applied for immobilization of enzyme to many different metal oxide catalysts coated with thermoresponsive polymers, mainly due to the versatility of dopamine chemistry. These novel intelligent bi-functional catalysts will be promising for applications in environmental science and biocatalyst fields, such as for the "one-pot" degradation of different organic pollutants in water treatment.

ASSOCIATED CONTENT

Supporting Information.

The Supporting Information is available free of charge on the ACS Publications website.

GC-MS spectra for the GA/DOPA-Br mixture, ^{1}H NMR spectra for the "one-pot" GA/NIPAM copolymerization and final poly(NIPAM)-*r*-(GA)-*r*-($PEGA_{480}$) product, SEC traces for the poly(NIPAM)-*r*-(GA) with different R_{co} values, turbidity for the TiO_2 hybrids, UV/Vis spectra for

the degradation of ABTS in the presence of laccase and degradation of BPA in the presence of TiO_2 nanoparticles under irradiation of simulated sunlight (PDF).

AUTHOR INFORMATION

Corresponding Author

* E-mail: zhangqiang@njust.edu.cn (Qiang Zhang).

ORCID

Qiang Zhang: 0000-0003-4596-9993

David M. Haddleton: 0000-0002-4965-0827

Author Contributions

The manuscript was written through contributions of all authors. All authors have given approval to the final version of the manuscript.

Funding Sources

Financial support from the Natural Science Foundation of China (21504044), Natural Science Foundation of Jiangsu Province (BK20150769), Fundamental Research Funds for the Central Universities (30916011203) and China Postdoctoral Science Foundation (157453) are greatly acknowledged.

Notes

The authors declare no competing financial interest.

ACKNOWLEDGMENT

This project was under financial support from the Natural Science Foundation of China (21504044), Natural Science Foundation of Jiangsu Province (BK20150769), Fundamental Research Funds for the Central Universities (30916011203) and China Postdoctoral Science Foundation (157453). Q. Z. appreciate the support from the Thousand Talents Plan and Jiangsu Innovation and Entrepreneurship Program.

REFERENCES

1. DiCosimo, R.; McAuliffe, J.; Poulose, A. J.; Bohlmann, G., Industrial use of immobilized enzymes. *Chem. Soc. Rev.* **2013,** *42*, (15), 6437-6474.
2. Franssen, M. C. R.; Steunenberg, P.; Scott, E. L.; Zuilhof, H.; Sanders, J. P. M., Immobilised enzymes in biorenewables production. *Chem. Soc. Rev.* **2013,** *42*, (15), 6491-6533.
3. Shoda, S.-i.; Uyama, H.; Kadokawa, J.-i.; Kimura, S.; Kobayashi, S., Enzymes as Green Catalysts for Precision Macromolecular Synthesis. *Chem. Rev.* **2016,** *116*, (4), 2307-2413.
4. Milczek, E. M., Commercial Applications for Enzyme-Mediated Protein Conjugation: New Developments in Enzymatic Processes to Deliver Functionalized Proteins on the Commercial Scale. *Chem. Rev.* **2018,** *118*, (1), 119-141.
5. Shi, J.; Jiang, Y.; Jiang, Z.; Wang, X.; Wang, X.; Zhang, S.; Han, P.; Yang, C., Enzymatic conversion of carbon dioxide. *Chem. Soc. Rev.* **2015,** *44*, (17), 5981-6000.
6. Sheldon, R. A.; van Pelt, S., Enzyme immobilisation in biocatalysis: why, what and how. *Chem. Soc. Rev.* **2013,** *42*, (15), 6223-6235.
7. Sheldon, R. A., Enzyme Immobilization: The Quest for Optimum Performance. *Adv. Synth. Catal.* **2007,** *349*, (8-9), 1289-1307.
8. Hanefeld, U.; Gardossi, L.; Magner, E., Understanding enzyme immobilisation. *Chem. Soc. Rev.* **2009,** *38*, (2), 453-468.
9. Goddard, J. M.; Hotchkiss, J. H., Polymer surface modification for the attachment of bioactive compounds. *Prog. Polym. Sci.* **2007,** *32*, (7), 698-725.
10. Credou, J.; Berthelot, T., Cellulose: from biocompatible to bioactive material. *J. Mater. Chem. B* **2014,** *2*, (30), 4767-4788.
11. Shin, Y. M.; Lee, Y. B.; Kim, S. J.; Kang, J. K.; Park, J.-C.; Jang, W.; Shin, H., Mussel-Inspired Immobilization of Vascular Endothelial Growth Factor (VEGF) for Enhanced Endothelialization of Vascular Grafts. *Biomacromolecules* **2012,** *13*, (7), 2020-2028.
12. Keller, D.; Beloqui, A.; Martínez-Martínez, M.; Ferrer, M.; Delaittre, G., Nitrilotriacetic Amine-Functionalized Polymeric Core–Shell Nanoparticles as Enzyme Immobilization Supports. *Biomacromolecules* **2017,** *18*, (9), 2777-2788.
13. Talbert, J. N.; Wang, L.-S.; Duncan, B.; Jeong, Y.; Andler, S. M.; Rotello, V. M.; Goddard, J. M., Immobilization and Stabilization of Lipase (CaLB) through Hierarchical Interfacial Assembly. *Biomacromolecules* **2014,** *15*, (11), 3915-3922.
14. Mateo, C.; Fernández-Lorente, G.; Abian, O.; Fernández-Lafuente, R.; Guisán, J. M., Multifunctional Epoxy Supports: A New Tool To Improve the Covalent Immobilization of Proteins. The Promotion of Physical Adsorptions of Proteins on the Supports before Their Covalent Linkage. *Biomacromolecules* **2000,** *1*, (4), 739-745.

15. Mateo, C.; Torres, R.; Fernández-Lorente, G.; Ortiz, C.; Fuentes, M.; Hidalgo, A.; López-Gallego, F.; Abian, O.; Palomo, J. M.; Betancor, L.; Pessela, B. C. C.; Guisan, J. M.; Fernández-Lafuente, R., Epoxy-Amino Groups: A New Tool for Improved Immobilization of Proteins by the Epoxy Method. *Biomacromolecules* **2003,** *4*, (3), 772-777.
16. Grazú, V.; Abian, O.; Mateo, C.; Batista-Viera, F.; Fernández-Lafuente, R.; Guisán, J. M., Novel Bifunctional Epoxy/Thiol-Reactive Support to Immobilize Thiol Containing Proteins by the Epoxy Chemistry. *Biomacromolecules* **2003,** *4*, (6), 1495-1501.
17. Chen, B.; Hu, J.; Miller, E. M.; Xie, W.; Cai, M.; Gross, R. A., Candida antarctica Lipase B Chemically Immobilized on Epoxy-Activated Micro- and Nanobeads: Catalysts for Polyester Synthesis. *Biomacromolecules* **2008,** *9*, (2), 463-471.
18. Mateo, C.; Palomo, J. M.; Fuentes, M.; Betancor, L.; Grazu, V.; López-Gallego, F.; Pessela, B. C. C.; Hidalgo, A.; Fernández-Lorente, G.; Fernández-Lafuente, R.; Guisán, J. M., Glyoxyl agarose: A fully inert and hydrophilic support for immobilization and high stabilization of proteins. *Enzyme Microb. Technol.* **2006,** *39*, (2), 274-280.
19. Li, D.; Teoh, W. Y.; Gooding, J. J.; Selomulya, C.; Amal, R., Functionalization Strategies for Protease Immobilization on Magnetic Nanoparticles. *Adv. Funct. Mater.* **2010,** *20*, (11), 1767-1777.
20. Mateo, C.; Grazu, V.; Palomo, J. M.; Lopez-Gallego, F.; Fernandez-Lafuente, R.; Guisan, J. M., Immobilization of enzymes on heterofunctional epoxy supports. *Nat. Protocols* **2007,** *2*, (5), 1022-1033.
21. Luo, X.; Zhang, L., Immobilization of Penicillin G Acylase in Epoxy-Activated Magnetic Cellulose Microspheres for Improvement of Biocatalytic Stability and Activities. *Biomacromolecules* **2010,** *11*, (11), 2896-2903.
22. Mateo, C.; Abian, O.; Fernandez‐Lafuente, R.; Guisan, J. M., Increase in conformational stability of enzymes immobilized on epoxy-activated supports by favoring additional multipoint covalent attachment☆. *Enzyme Microb. Technol.* **2000,** *26*, (7), 509-515.
23. Wheatley, J. B.; Schmidt Jr, D. E., Salt-induced immobilization of affinity ligands onto epoxide-activated supports. *J. Chromatogr. A* **1999,** *849*, (1), 1-12.
24. Barbosa, O.; Torres, R.; Ortiz, C.; Berenguer-Murcia, Á.; Rodrigues, R. C.; Fernandez-Lafuente, R., Heterofunctional Supports in Enzyme Immobilization: From Traditional Immobilization Protocols to Opportunities in Tuning Enzyme Properties. *Biomacromolecules* **2013,** *14*, (8), 2433-2462.
25. Lei, Z.; Gao, J.; Liu, X.; Liu, D.; Wang, Z., Poly(glycidyl methacrylate-co-2-hydroxyethyl methacrylate) Brushes as Peptide/Protein Microarray Substrate for Improving Protein Binding and Functionality. *ACS Appl. Mater. Interfaces* **2016,** *8*, (16), 10174-10182.
26. Guo, B.; Yuan, J.; Gao, Q., Preparation and characterization of temperature and pH-sensitive chitosan material and its controlled release on coenzyme A. *Colloids and Surfaces B: Biointerfaces* **2007,** *58*, (2), 151-156.
27. Peng, H.; Rübsam, K.; Jakob, F.; Pazdzior, P.; Schwaneberg, U.; Pich, A., Reversible Deactivation of Enzymes by Redox-Responsive Nanogel Carriers. *Macromol. Rapid. Commun.* **2016,** *37*, (21), 1765-1771.
28. Yuba, E.; Yamaguchi, A.; Yoshizaki, Y.; Harada, A.; Kono, K., Bioactive polysaccharide-based pH-sensitive polymers for cytoplasmic delivery of antigen and activation of antigen-specific immunity. *Biomaterials* **2017,** *120*, 32-45.

29. Huang, X.; Appelhans, D.; Formanek, P.; Simon, F.; Voit, B., Tailored Synthesis of Intelligent Polymer Nanocapsules: An Investigation of Controlled Permeability and pH-Dependent Degradability. *ACS Nano* **2012,** *6*, (11), 9718-9726.
30. Zhou, L.; Chen, Z.; Dong, K.; Yin, M.; Ren, J.; Qu, X., DNA-mediated Construction of Hollow Upconversion Nanoparticles for Protein Harvesting and Near-Infrared Light Triggered Release. *Adv. Mater.* **2014,** *26*, (15), 2424-2430.
31. Xie, Y.; Jiang, S.; Xia, F.; Hu, X.; He, H.; Yin, Z.; Qi, J.; Lu, Y.; Wu, W., Glucan microparticles thickened with thermosensitive gels as potential carriers for oral delivery of insulin. *J. Mater. Chem. B* **2016,** *4*, (22), 4040-4048.
32. Dyal, A.; Loos, K.; Noto, M.; Chang, S. W.; Spagnoli, C.; Shafi, K. V. P. M.; Ulman, A.; Cowman, M.; Gross, R. A., Activity of Candida rugosa Lipase Immobilized on γ-Fe2O3 Magnetic Nanoparticles. *J. Am. Chem. Soc.* **2003,** *125*, (7), 1684-1685.
33. Jiang, D.-S.; Long, S.-Y.; Huang, J.; Xiao, H.-Y.; Zhou, J.-Y., Immobilization of Pycnoporus sanguineus laccase on magnetic chitosan microspheres. *Biochem. Eng. J.* **2005,** *25*, (1), 15-23.
34. Li, Y.; Huang, G.; Zhang, X.; Li, B.; Chen, Y.; Lu, T.; Lu, T. J.; Xu, F., Magnetic Hydrogels and Their Potential Biomedical Applications. *Adv. Funct. Mater.* **2013,** *23*, (6), 660-672.
35. Wang, W.; Xu, Y.; Wang, D. I. C.; Li, Z., Recyclable Nanobiocatalyst for Enantioselective Sulfoxidation: Facile Fabrication and High Performance of Chloroperoxidase-Coated Magnetic Nanoparticles with Iron Oxide Core and Polymer Shell. *J. Am. Chem. Soc.* **2009,** *131*, (36), 12892-12893.
36. Yuan, S.; Wan, D.; Liang, B.; Pehkonen, S. O.; Ting, Y. P.; Neoh, K. G.; Kang, E. T., Lysozyme-Coupled Poly(poly(ethylene glycol) methacrylate)−Stainless Steel Hybrids and Their Antifouling and Antibacterial Surfaces. *Langmuir* **2011,** *27*, (6), 2761-2774.
37. Huang, J.; Li, X.; Zheng, Y.; Zhang, Y.; Zhao, R.; Gao, X.; Yan, H., Immobilization of Penicillin G Acylase on Poly[(glycidyl methacrylate)-co-(glycerol monomethacrylate)]-Grafted Magnetic Microspheres. *Macromol. Biosci.* **2008,** *8*, (6), 508-515.
38. Yakup Arica, M.; Soydogan, H.; Bayramoglu, G., Reversible immobilization of Candida rugosa lipase on fibrous polymer grafted and sulfonated p(HEMA/EGDMA) beads. *Bioprocess Biosyst. Eng.* **2010,** *33*, (2), 227-236.
39. Nie, J.-J.; Zhao, W.; Hu, H.; Yu, B.; Xu, F.-J., Controllable Heparin-Based Comb Copolymers and Their Self-assembled Nanoparticles for Gene Delivery. *ACS Appl. Mater. Interfaces* **2016,** *8*, (13), 8376-8385.
40. Wang, R.; Hu, Y.; Zhao, N.; Xu, F.-J., Well-Defined Peapod-like Magnetic Nanoparticles and Their Controlled Modification for Effective Imaging Guided Gene Therapy. *ACS Appl. Mater. Interfaces* **2016,** *8*, (18), 11298-11308.
41. Wu, Y.; Wang, A.; Ding, X.; Xu, F.-J., Versatile Functionalization of Poly(methacrylic acid) Brushes with Series of Proteolytically Cleavable Peptides for Highly Sensitive Protease Assay. *ACS Appl. Mater. Interfaces* **2017,** *9*, (1), 127-135.
42. Wu, Y.; Nizam, M. N.; Ding, X.; Xu, F.-J., Rational Design of Peptide-Functionalized Poly(Methacrylic Acid) Brushes for On-Chip Detection of Protease Biomarkers. *ACS Biomaterials Science & Engineering* **2017**, DOI: 10.1021/acsbiomaterials.7b00584.
43. Zhang, Q.; Shen, C.; Zhao, N.; Xu, F. J., Redox‐Responsive and Drug‐Embedded Silica Nanoparticles with Unique Self‐Destruction Features for Efficient Gene/Drug Codelivery. *Adv. Funct. Mater.* **2017,** *27*, (10), 1606229.

44. Zhang, Q.; Nurumbetov, G.; Simula, A.; Zhu, C.; Li, M.; Wilson, P.; Kempe, K.; Yang, B.; Tao, L.; Haddleton, D. M., Synthesis of well-defined catechol polymers for surface functionalization of magnetic nanoparticles. *Polym. Chem.* **2016,** *7*, (45), 7002-7010.
45. Wang, D.; Guo, S.; Zhang, Q.; Wilson, P.; Haddleton, D. M., Mussel-inspired thermoresponsive polymers with a tunable LCST by Cu(0)-LRP for the construction of smart TiO2 nanocomposites. *Polym. Chem.* **2017,** *8*, (24), 3679-3688.
46. Basuki, J. S.; Esser, L.; Duong, H. T. T.; Zhang, Q.; Wilson, P.; Whittaker, M. R.; Haddleton, D. M.; Boyer, C.; Davis, T. P., Magnetic nanoparticles with diblock glycopolymer shells give lectin concentration-dependent MRI signals and selective cell uptake. *Chemical Science* **2014,** *5*, (2), 715-726.
47. Guo, S.; Zhang, Q.; Wang, D.; Wang, L.; Lin, F.; Wilson, P.; Haddleton, D. M., Bioinspired coating of TiO2 nanoparticles with antimicrobial polymers by Cu(0)-LRP: grafting to vs. grafting from. *Polym. Chem.* **2017,** *8*, (42), 6570-6580.
48. Kim, M. I.; Shim, J.; Li, T.; Woo, M.-A.; Cho, D.; Lee, J.; Park, H. G., Colorimetric quantification of galactose using a nanostructured multi-catalyst system entrapping galactose oxidase and magnetic nanoparticles as peroxidase mimetics. *Analyst* **2012,** *137*, (5), 1137-1143.
49. Kim, M. I.; Ye, Y.; Won, B. Y.; Shin, S.; Lee, J.; Park, H. G., A Highly Efficient Electrochemical Biosensing Platform by Employing Conductive Nanocomposite Entrapping Magnetic Nanoparticles and Oxidase in Mesoporous Carbon Foam. *Adv. Funct. Mater.* **2011,** *21*, (15), 2868-2875.
50. Vennestrøm, P. N. R.; Christensen, C. H.; Pedersen, S.; Grunwaldt, J.-D.; Woodley, J. M., Next-Generation Catalysis for Renewables: Combining Enzymatic with Inorganic Heterogeneous Catalysis for Bulk Chemical Production. *ChemCatChem* **2010,** *2*, (3), 249-258.
51. Li, H.; Fang, Z.; Smith, R. L.; Yang, S., Efficient valorization of biomass to biofuels with bifunctional solid catalytic materials. *Progr. Energy Combust. Sci.* **2016,** *55*, 98-194.
52. Vennestrøm, P. N. R.; Taarning, E.; Christensen, C. H.; Pedersen, S.; Grunwaldt, J.-D.; Woodley, J. M., Chemoenzymatic Combination of Glucose Oxidase with Titanium Silicalite-1. *ChemCatChem* **2010,** *2*, (8), 943-945.
53. Chen, X.; Mao, S. S., Titanium Dioxide Nanomaterials: Synthesis, Properties, Modifications, and Applications. *Chem. Rev.* **2007,** *107*, (7), 2891-2959.
54. Chong, M. N.; Jin, B.; Chow, C. W. K.; Saint, C., Recent developments in photocatalytic water treatment technology: A review. *Water Res.* **2010,** *44*, (10), 2997-3027.
55. Li, Q.; Mahendra, S.; Lyon, D. Y.; Brunet, L.; Liga, M. V.; Li, D.; Alvarez, P. J. J., Antimicrobial nanomaterials for water disinfection and microbial control: Potential applications and implications. *Water Res.* **2008,** *42*, (18), 4591-4602.
56. Duran, N.; Esposito, E., Potential applications of oxidative enzymes and phenoloxidase-like compounds in wastewater and soil treatment: a review. *Applied Catalysis B-Environmental* **2000,** *28*, (2), 83-99.
57. Riva, S., Laccases: blue enzymes for green chemistry. *Trends Biotechnol.* **2006,** *24*, (5), 219-226.
58. Couto, S. R.; Herrera, J. L. T., Industrial and biotechnological applications of laccases: A review. *Biotechnol. Adv.* **2006,** *24*, (5), 500-513.
59. Hou, J.; Dong, G.; Ye, Y.; Chen, V., Laccase immobilization on titania nanoparticles and titania-functionalized membranes. *J. Membr. Sci.* **2014,** *452*, 229-240.
60. Ciampolini, M.; Nardi, N., Five-Coordinated High-Spin Complexes of Bivalent Cobalt, Nickel, andCopper with Tris(2-dimethylaminoethyl)amine. *Inorg. Chem.* **1966,** *5*, (1), 41-44.

61. Queffelec, J.; Gaynor, S. G.; Matyjaszewski, K., Optimization of Atom Transfer Radical Polymerization Using Cu(I)/Tris(2-(dimethylamino)ethyl)amine as a Catalyst. *Macromolecules* **2000,** *33*, (23), 8629-8639.
62. Zhang, Q.; Anastasaki, A.; Li, G.-Z.; Haddleton, A. J.; Wilson, P.; Haddleton, D. M., Multiblock sequence-controlled glycopolymers via Cu(0)-LRP following efficient thiol-halogen, thiol-epoxy and CuAAC reactions. *Polym. Chem.* **2014,** *5*, (12), 3876-3883.
63. Nguyen, T.; Francis, M. B., Practical Synthetic Route to Functionalized Rhodamine Dyes. *Org. Lett.* **2003,** *5*, (18), 3245-3248.
64. Zhang, Q.; Wilson, P.; Li, Z.; McHale, R.; Godfrey, J.; Anastasaki, A.; Waldron, C.; Haddleton, D. M., Aqueous Copper-Mediated Living Polymerization: Exploiting Rapid Disproportionation of CuBr with Me6TREN. *J. Am. Chem. Soc.* **2013,** *135*, (19), 7355-7363.
65. Pich, A.; Bhattacharya, S.; Adler, H. J.; Wage, T.; Taubenberger, A.; Li, Z.; van Pee, K. H.; Bohmer, U.; Bley, T., Composite magnetic particles as carriers for laccase from Trametes versicolor. *Macromolecular bioscience* **2006,** *6*, (4), 301-10.
66. Dai, Y.; Niu, J.; Liu, J.; Yin, L.; Xu, J., In situ encapsulation of laccase in microfibers by emulsion electrospinning: preparation, characterization, and application. *Bioresource technology* **2010,** *101*, (23), 8942-7.
67. De, S.; Khan, A., Efficient synthesis of multifunctional polymersviathiol-epoxy "click" chemistry. *Chem. Commun.* **2012,** *48*, (25), 3130-3132.
68. Tsarevsky, N. V.; Bencherif, S. A.; Matyjaszewski, K., Graft Copolymers by a Combination of ATRP and Two Different Consecutive Click Reactions. *Macromolecules* **2007,** *40*, (13), 4439-4445.
69. Zhang, Q.; Slavin, S.; Jones, M. W.; Haddleton, A. J.; Haddleton, D. M., Terminal functional glycopolymers via a combination of catalytic chain transfer polymerisation (CCTP) followed by three consecutive click reactions. *Polym. Chem.* **2012,** *3*, (4), 1016-1023.
70. Prolongo, S. G.; Prolongo, G., Epoxy/poly(4-vinylphenol)blends crosslinked by imidazole initiation. *J. Therm. Anal. Calorim.* **2007,** *87*, (1), 259-268.
71. Jost, S.; Vanbellinghen, L.; Henderson, P.; Marchand-Brynaert, J., Reaction of bisphenol-A diglycidyl ether with substituted phenols. *Org. Prep. Proced. Int.* **1999,** *31*, (2), 193-200.
72. Seth, K.; Roy, S. R.; Pipaliya, B. V.; Chakraborti, A. K., Synergistic dual activation catalysis by palladium nanoparticles for epoxide ring opening with phenols. *Chem. Commun.* **2013,** *49*, (52), 5886-5888.
73. Huang, Y. P.; Woo, E. M., Physical miscibility and chemical reactions between diglycidylether of bisphenol-A epoxy and poly(4-vinyl phenol). *Polymer* **2002,** *43*, (25), 6795-6804.
74. Limer, A.; Haddleton, D. M., Amide Functional Initiators for Transition-Metal-Mediated Living Radical Polymerization. *Macromolecules* **2006,** *39*, (4), 1353-1358.
75. Nagaveni, K.; Sivalingam, G.; Hegde, M. S.; Madras, G., Photocatalytic Degradation of Organic Compounds over Combustion-Synthesized Nano-TiO2. *Environ. Sci. Technol.* **2004,** *38*, (5), 1600-1604.
76. Guo, C.; Ge, M.; Liu, L.; Gao, G.; Feng, Y.; Wang, Y., Directed Synthesis of Mesoporous TiO2 Microspheres: Catalysts and Their Photocatalysis for Bisphenol A Degradation. *Environ. Sci. Technol.* **2010,** *44*, (1), 419-425.
77. Hsu, C.-A.; Wen, T.-N.; Su, Y.-C.; Jiang, Z.-B.; Chen, C.-W.; Shyur, L.-F., Biological Degradation of Anthroquinone and Azo Dyes by a Novel Laccase from Lentinus sp. *Environ. Sci. Technol.* **2012,** *46*, (9), 5109-5117.

78. Yin, L.; Shen, Z.; Niu, J.; Chen, J.; Duan, Y., Degradation of Pentachlorophenol and 2,4-Dichlorophenol by Sequential Visible-Light Driven Photocatalysis and Laccase Catalysis. *Environ. Sci. Technol.* **2010,** *44*, (23), 9117-9122.
79. Zheng, D.; Wang, N.; Wang, X.; Tang, Y.; Zhu, L.; Huang, Z.; Tang, H.; Shi, Y.; Wu, Y.; Zhang, M.; Lu, B., Effects of the interaction of TiO2 nanoparticles with bisphenol A on their physicochemical properties and in vitro toxicity. *J. Hazard. Mater.* **2012,** *199*, (Supplement C), 426-432.

Table of Contents Graphic